4-Quinolone Derivatives: High-Affinity Ligands at the Benzodiazepine Site of Brain GABA$_A$ Receptors. Synthesis, Pharmacology, and Pharmacophore Modeling

Erik Lager,[†] Pierre Andersson,[†] Jakob Nilsson,[†] Ingrid Pettersson,[||] Elsebet Østergaard Nielsen,[§] Mogens Nielsen,[‡] Olov Sterner,[†] and Tommy Liljefors*,[‡]

Department of Organic Chemistry, Lund University, P.O.B. 124, SE−221 00 Lund, Sweden, Department of Medicinal Chemistry, The Danish University of Pharmaceutical Sciences, Universitetsparken 2, DK-2100 Copenhagen, Denmark, NeuroSearch A/S, DK-2750 Ballerup, Denmark, and Novo Nordisk A/S, Novo Nordisk Park, DK-2760 Måløv, Denmark

The 3-ethoxycarbonyl-4-quinolone compound **1** has previously been identified via a database search as an interesting lead compound for ligand binding at the benzodiazepine site of GABA$_A$ receptors (Kahnberg et al. *J. Mol. Graphics Modelling* **2004**, *23*, 253−261). Pharmacophore-guided optimization of this lead compound yielded a number of high-affinity ligands for the benzodiazepine site including compounds **20** and **23**−**25** displaying sub-nanomolar affinities. A few of the compounds have been tested on the α$_1$β$_2$γ$_{2S}$ and α$_3$β$_2$γ$_{2S}$ GABA$_A$ receptor subtypes, and two of the compounds (**5** and **19**) display selectivity for α$_1$- versus α$_3$-containing receptors by a factor of 22 and 27, respectively. This selectivity for α$_1$β$_2$γ$_{2S}$ is in the same range as that for the well-known α$_1$ subunit selective compound zolpidem.

Introduction

γ-Aminobutyric acid, GABA, is one of the major inhibitory neurotransmitters in the central nervous system and exerts its physiological effect by binding to three different receptor types in the neuronal membrane: GABA$_A$, GABA$_B$, and GABA$_C$ receptors.[1] GABA$_B$ belongs to the family of G-protein-coupled receptors and act via intracellular second messengers.[2] GABA$_A$[3] and GABA$_C$[4] are coupled directly to anion channels and cause an increase in chloride permeability of the membrane. Mammalian brain GABA$_A$ receptors have been shown to be heteropentameric assemblies of protein subunits from seven different classes with multiple isoforms (α$_{1-6}$, β$_{1-4}$, γ$_{1-4}$, δ, ε, π, and ρ$_1$-ρ$_3$), each encoded by different genes.[5] Most GABA$_A$ receptors are composed of two α-, two β-, and one γ-subunit. It is believed that receptors with different subtype composition can give rise to different physiological effects, e.g. α$_1$-containing receptors are implicated in sedation and anterograde amnesia, and α$_2$-, α$_3$-, or possibly α$_5$-containing receptors in anxiolytic activity.[6,7] Benzodiazepines, β-carbolines, barbiturates, ethanol, and certain steroids are the best known ligands that allosterically modify the chloride channel gating effect of GABA on GABA$_A$ receptors.[1]

The most important drugs in clinical use for GABA$_A$ receptor modulating purposes are the benzodiazepines, which mainly give anxiolytic, anticonvulsant, muscle relaxant, and sedative-hypnotic effects.[8] Many classes of compounds bind to the same binding site as the benzodiazepines, e.g. β-carbolines, triazolopyridazines, pyrazoloquinolinones, cyclopyrrolones, pyridodiindoles, quinolines, and flavones.[9−12]

Cook and co-workers[13] have developed a comprehensive pharmacophore model for the benzodiazepine receptor based on structure−activity relationship studies of 136 different ligands from 10 structurally different classes of compounds. The model was developed assuming that benzodiazepine receptor agonists, antagonists, and inverse agonists all share the same binding pocket. Recent research with synthetic flavone derivatives led to a further development of the pharmacophore model.[11,12] The model was subsequently used for identification of novel lead structures by a 3D database search using the program Catalyst.[14] One of the hits identified was the 4-quinolone **1** (Table 1) which displayed the highest affinity of the purchased and tested compounds (K_i = 122 nM).[14] In the present work we have performed pharmacophore-guided optimization of this lead structure. In addition to compounds derived from **1**, a few pyrazolopyrimidinones based on another hit obtained in the database search mentioned above were also synthesized and tested.

Results and Discussion

Chemistry. The structures of the compounds investigated in this study are shown in Table 1. The 4-quinolones were synthesized according to procedures previously described[15] by a condensation of an appropriate aniline with either diethyl ethoxymethylenemalonate or diethyl acetylmalonate followed by cyclization of the intermediate upon reflux in diphenyl ether (Scheme 1). The alkyl group (R$_1$) was varied by transesterification using different alcohols. Initially *p*-toluenesulfonic acid was used as a catalyst for this reaction, but the corresponding acid **13** was obtained as a side product which hampered the purifying process. The use of titanium(IV) isopropoxide as a catalyst[16] gave cleaner reactions without the need to use dried solvents. This procedure also worked well with secondary alcohols and primary amines.

The pyrazolopyrimidinones were synthesized according to previously described procedures,[17] utilizing a one-pot procedure which includes the condensation of 3-aminopyrazole and ethoxymethylenemalonate followed by cyclization of the intermediate. The alkyl chain was subsequently varied, by transesterification with *n*-propanol using titanium(IV) isopropoxide as a catalyst (Scheme 2).

Receptor Binding. Table 1 shows that the tested 4-quinolones inhibit the specific binding of ^{3}H-flumazenil with a range of K_i values from low or sub-nM (**3**, **19**, **20**, **23**−**25**) to μM concentrations. Compound **25** displays the highest affinity in
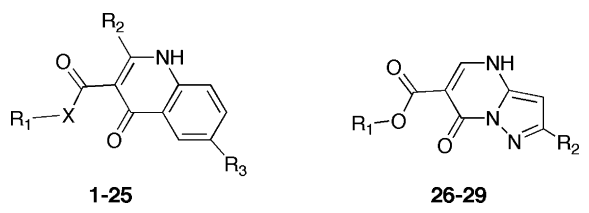
* To whom correspondence should be sent. Tel. +45-35 30 65 05. E-mail: tl@dfuni.dk. Fax: +45−35 30 60 40.
† Lund University.
‡ The Danish University of Pharmaceutical Sciences.
§ NeuroSearch A/S.
|| Novo Nordisk A/S.

Table 1. K_i Values of 4-Quinolones and Pyrazolopyrimidinones Tested on ^{3}H-Flumazenil Binding in Vitro to Rat Cortical Membranes

compd	R$_1$	R$_2$	R$_3$	X	K_i value (nM)^a
1	CH$_2$CH$_3$	H	CF$_3$	O	122 ± 46
2	CH$_2$CH$_3$	H	CH$_2$CH$_3$	O	20 ± 5
3	CH$_2$CH$_2$CH$_3$	H	CH$_2$CH$_3$	O	1.8 ± 0.3
4	CH$_2$CH$_2$CH$_2$CH$_3$	H	CH$_2$CH$_3$	O	13 ± 4
5	CH$_2$CH$_2$CH(CH$_3$)$_2$	H	CH$_2$CH$_3$	O	28 ± 8
6	CH$_2$CH(CH$_3$)CH$_2$CH$_3$	H	CH$_2$CH$_3$	O	28 ± 6
7	CH$_2$CH$_2$CH$_2$CH$_2$CH$_3$	H	CH$_2$CH$_3$	O	35 ± 8
8	CH$_2$CH(CH$_2$CH$_3$)$_2$	H	CH$_2$CH$_3$	O	92 ± 13
9	cyclopentyl	H	CH$_2$CH$_3$	O	19 ± 4
10	CH(CH$_3$)$_2$	H	CH$_2$CH$_3$	O	214 ± 10
11	CH(CH$_3$)CH$_2$CH(CH$_3$)$_2$	H	CH$_2$CH$_3$	O	295 ± 17
12	CH(CH$_2$CH$_3$)$_2$	H	CH$_2$CH$_3$	O	2600 ± 570
13	H	H	CH$_2$CH$_3$	O	208 ± 53
14	CH$_2$CH$_3$	H	H	O	78 ± 10
15	CH$_2$CH$_2$CH$_2$CH$_3$	H	H	O	54 ± 45
16	CH$_2$CH$_3$	H	Br	O	16 ± 5
17	CH$_2$CH$_3$	H	CH$_2$CH$_2$CH$_3$	O	17 ± 0.5
18	CH$_2$CH$_3$	H	CH(CH$_3$)$_2$	O	15 ± 4
19	CH$_2$CH$_3$	H	CH$_2$C$_6$H$_5$	O	1.4 ± 0.2
20	CH$_2$CH$_2$CH$_3$	H	CH$_2$C$_6$H$_5$	O	0.17 ± 0.01
21	CH$_2$CH$_3$	CH$_3$	CH$_2$CH$_3$	O	6850 ± 1900
22	CH$_2$CH$_3$	CH$_3$	Br	O	4200 ± 560
23	CH$_2$CH$_2$CH$_3$	H	CH$_2$CH$_3$	NH	0.26 ± 0.03
24	CH$_2$CH$_2$CH$_2$CH$_3$	H	CH$_2$CH$_3$	NH	0.54 ± 0.06
25	CH$_2$CH$_2$CH$_3$	H	CH$_2$C$_6$H$_5$	NH	0.048 ± 0.006
26	CH$_2$CH$_3$	CH$_3$			>10000
27	CH$_2$CH$_2$CH$_3$	CH$_3$			870 ± 285
28	CH$_2$CH$_3$	H			>10000
29	CH$_2$CH$_2$CH$_3$	H			7130 ± 4200

^{a} Each K_i value is the mean ± SD of three determinations.

Scheme 1^a
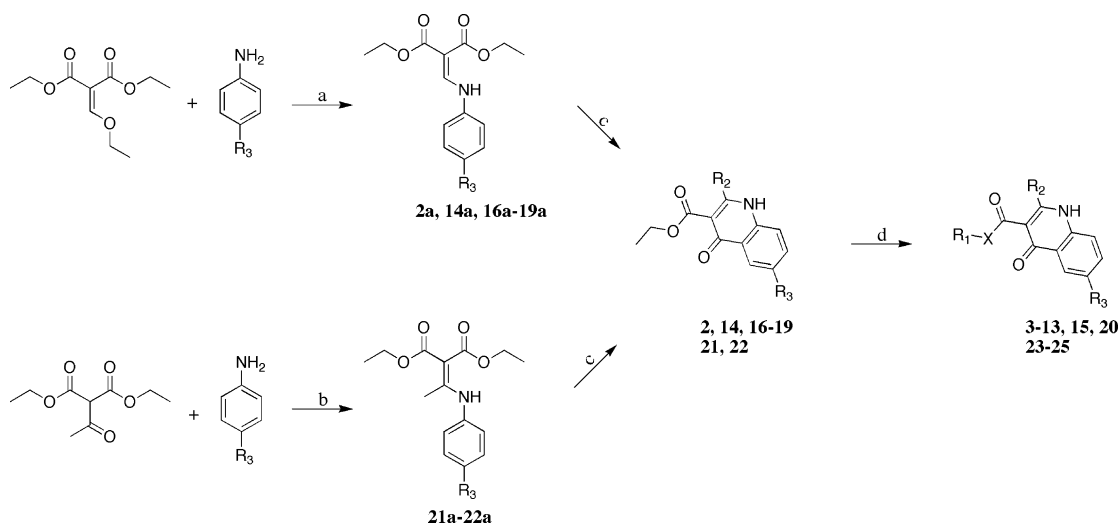
^{a} Reagents and conditions: (a) neat, 130 °C, 2 h; (b) *p*-TsOH, pentane, reflux (Dean−Stark trap), 24 h; (c) diphenyl ether, reflux, 1 h; (d) *p*-TsOH or Ti(O-*i*-Pr)$_4$, alcohol or amine, reflux overnight.

the present series of compounds with a K_i value of 0.048 nM. The results show that amide derivatives (**23**−**25**) display higher affinities than the corresponding esters (**3**, **4**, and **20**). The pyrazolopyrimidinones (**26**−**29**) inhibited the specific binding of ^{3}H-flumazenil in μM concentrations.

Fitting to the Pharmacophore Model. The pharmacophore model for the benzodiazepine site, developed by Cook and co-

workers[13] and previously validated and further refined by us using the results of structure−activity studies for a series of flavonoids, [11,12] is shown in Figure 1a. The figure displays the interactions between the high-affinity flavonoid 5′-bromo-2′-hydroxy-6-methylflavone (K_i = 0.9 nM[12]) and the sites of the pharmacophore model. H1 and A2 are hydrogen bond donating and hydrogen bond accepting sites, respectively. H2/A3 repre-

Scheme 2[a]
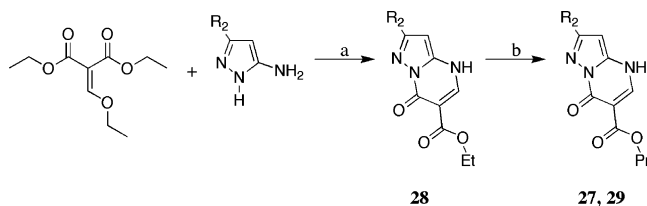
[a] Reagents and conditions: (a) neat, 200 °C, 10 min; (b) Ti(O-*i*-Pr)$_4$ and *n*-propanol, reflux, overnight.

sents a bifunctional site with the ability to act as a hydrogen bond donor as well as an acceptor. L1–L3 are lipophilic sites and S1–S5 denote regions of steric repulsive ligand–receptor interactions (receptor essential volumes). The term "interface" is used to denote a partly lipophilic region in the vicinity of the 5′-position in the flavone series. This region has been proposed to represent the interface between an α- and a γ- subunit in the GABA$_A$ receptor.[12] Figure 1b shows the proposed binding mode of the lead structure **1** in the pharmacophore model, and Figure 2 displays a superimposition of 5′-bromo-2′-hydroxy-6-methylflavone and **1** fitted to the pharmacophore model. As shown in Figure 1b, the ester and the ring carbonyl groups of **1** interact in a coplanar arrangement with H1 and H2, respectively, and the NH group forms a hydrogen bond with the A2 site corresponding to the hydrogen bond involving the 2′-OH group in the flavones (Figure 1a). The 6-CF$_3$ group of **1** coincides with the 5′-bromo substituent in the flavone. Substitution in this position in flavone derivatives by small substituents has previously been shown to give a significant increase in affinity.[11,12]

The proposed bioactive conformation of **1** in Figure 1b does not correspond to the global energy minimum conformation of the compound in aqueous solution. Conformational analysis using the MMFF94s force field and the GB/SA hydration model and performed as described in the Experimental Section indicates that the lowest energy conformation of **1** has parallel carbonyl groups with a 13° twist of the ester group with respect to the bicyclic ring system. In contrast, the carbonyl groups in the proposed bioactive conformation point at different directions as shown in Figure 3. However, the proposed binding conformation of **1** is calculated to be only 0.1 kcal/mol higher in energy than that of the calculated global energy minimum. All 4-quinolone esters in Table 1 except compounds **21** and **22** can adopt the proposed binding conformation with low conformational energy penalties, 0.1–0.3 kcal/mol. For the 2-methyl-substituted compounds **21** and **22**, the energy cost for adopting the proposed bioactive arrangement of the carbonyl groups is calculated to be significantly higher, 3.1 kcal/mol. The calculated lowest energy conformation of these compounds displays a 63° twist of the ester group with respect to the bicyclic ring. Steric repulsive interactions between the 2-methyl group and the ester carbonyl in the proposed bioactive conformation prevent the carbonyl groups to adopt a coplanar conformation with a low conformational energy penalty as required by the pharmacophore model. The calculated conformational energy penalty rationalizes the reduced affinities of **21** and **22** by a factor of 300 compared to **2** and **16**, respectively (Table 1). This is in accordance with previous conclusions that a planar or close to planar geometry of the core part of the ligand is required for high-affinity binding to the benzodiazepine receptor.[11,13] For the pyrazolo-pyrimidinones **26**–**29**, the energy difference between the lowest energy minimum and the proposed binding conformation is calculated to be 0.1 kcal/mol. In contrast to the conformational properties of compounds **1**–**22** and **26**–

29, conformational analysis of the amides **23**–**25** indicates that for these compounds the proposed binding conformation with respect to carbonyl arrangement is the global energy minimum conformation. This is due to stabilization of the proposed bioactive conformation by an intramolecular NH‑ ‑ ‑O=C hydrogen bond. The amides **23**–**25** display significantly higher affinities than the corresponding esters **3**, **4**, and **20** (Table 1). The differences in conformational energy penalties between the esters and the amides for adopting the bioactive conformation is too small (0.1–0.3 kcal/mol) to fully explain these affinity differences. The major reason for the higher affinities of the amide compounds compared to the esters is most probably due to the higher electron density of an amide carbonyl oxygen compared to that of an ester carbonyl oxygen. This makes the hydrogen bond interactions with the H1 site stronger for the amide compounds. It is also possible that the NH group of the amides have additional interactions with the A3 part of the H2/A3 site.

3-Carboxamide-4-quinolones have previously in a patent application been disclosed as GABA$_A$ brain receptor ligands.[18]

Interactions in the Lipophilic L1 and L2 Regions. Figures 1 and 2 clearly demonstrate that the ethyl ester group of lead structure **1** does not fill out the lipophilic regions L1 and in particular L2. It should be noted that the 6-methyl group in the flavone series (Figures 1a) increases the affinity by a factor of 23 and that the corresponding 6-ethyl, 6-propyl, and 6-isopropyl compounds in the flavone series also have significantly higher affinities than the 6-unsubstituted parent compound.[11,12] Therefore, a series of alkyl esters with different alkyl chain length and alkyl branching (**3**–**12**) was synthesized and tested in order to further explore the dimensions and other properties of the L2 region. The parent compound for this series is the 6-ethyl compound **2** which displays 6 times higher affinity than the lead compound **1**.

Extending the ester ethyl group in **2** to a propyl group in **3** increases the affinity by a factor of 11 (Table 1), only slightly lower than the effect on the affinity by a 6-methyl group in the flavone series mentioned above. As can be inferred from Figure 2, the methyl group of the ester propyl group in **3** coincides with the 6-methyl group in the flavonoids. Further chain elongations from propyl to butyl (**4**) and pentyl (**7**) result in affinities similar to that of **2** but to a significant reduction of affinity compared to the propylester **3**. The *N*-propyl amide **23** also has a somewhat higher affinity than the *N*-butyl amide **24**. Thus, with respect to alkyl chain length the propyl group is clearly optimal.

By analyzing the branched alkyl esters (**5**, **6**, **8**–**12**) as alkyl (methyl or ethyl) substituted ethyl, propyl, or butyl esters, Table 1 shows that despite higher lipophilicities, the branched alkyl esters display affinities which are lower than those of their parent straight chain alkyl esters. This indicates the presence of steric repulsions with the receptor in the L2 site and/or significant differences in the conformational energies required to adopt the bioactive conformations. The γ-branched alkyl ester **5** displays only a slightly lower affinity than the straight chain butyl ester **4**. This is also the case for the β-branched compound **6** if its ester alkyl group is analyzed as a methyl-substitued butyl group (**6** vs **4**). However, if it is analyzed as an ethyl-substituted propyl group the affinity decrease is 16-fold (**6** vs **3**). The β-branched alkyl group in **8** decreases the affinity by a factor of 7 compared to that of **4**.

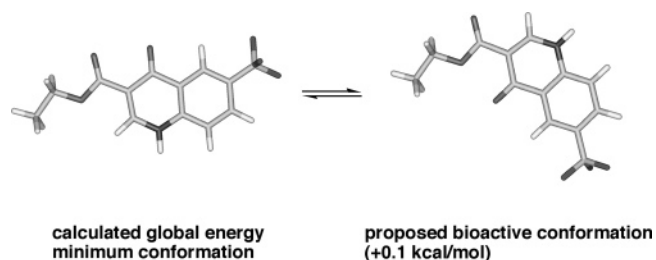The large variation in affinities for the compounds with α-branched alkyl groups (**9**–**12**) cannot be understood in terms of lipophilicity (**11** and **12** have high lipophilicities but low
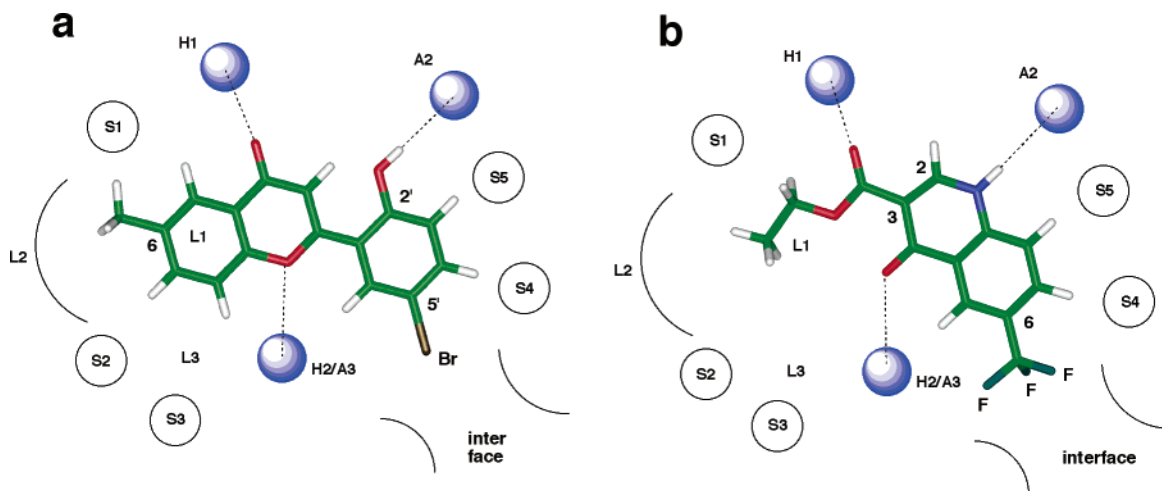
Figure 1. Binding modes of (a) the high-affinity flavonoid 5′-bromo-2′-hydroxy-6-methylflavone and (b) the lead compound **1** in the pharmacophore model.
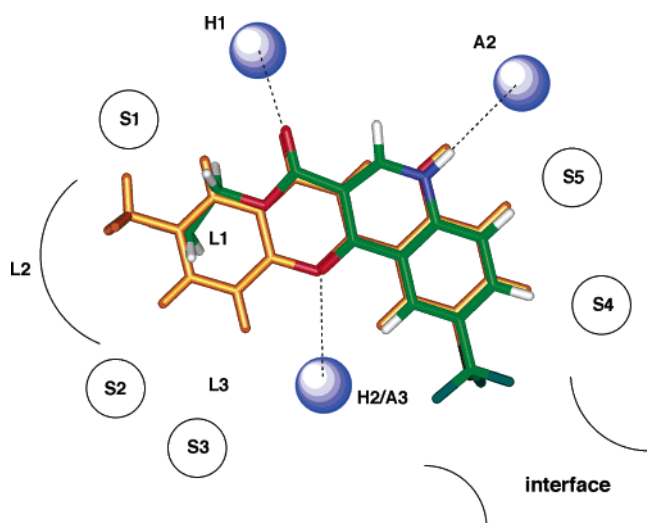
Figure 2. A molecular superimposition of the high-affinity flavonoid 5′-bromo-2′-hydroxy-6-methylflavone (orange carbon atoms) and the lead compound **1** (green carbon atoms) in the pharmacophore model.

calculated global energy minimum conformation

proposed bioactive conformation (+0.1 kcal/mol)

Figure 3. Conformational equilibrium with respect to arrangement of the carbonyl groups in the lead compound **1**.

affinities) or steric bulk (**10** is smaller than **9** but has a lower affinity). In an attempt to understand the origin of the significant affinity differences for the α-branched compounds, we have performed conformational analysis for **9**, **10**, and **12**. According to the pharmacophore model (Figure 1b), the ester ethyl in **2** as well as the propyl group in **3** display an all-anti (extended) bioactive conformation with the alkyl carbon atoms in the same plane as the ester carbonyl and the ring system. We have assumed that in the bioactive conformations of **9**, **10**, and **12**, one branch of the chain has an all-anti conformation superimposable on an all-anti ethyl or propyl group. To calculate the energy required for adopting the assumed bioactive conforma-

tion, two conformational searches were performed both with the carbonyl groups constrained to their proposed bioactive arrangement. In the first conformational search, no additional constraints were made. In the second search, one of the ester alkyl branches was additionally constrained to adopt an all-anti conformation whereas the other branch was allowed to find its energetically preferred conformation. The energy of lowest energy conformation found in the first search was then in each case subtracted from the energy of lowest energy conformation found in the second search. This gives the lowest possible conformational energies required for the ester alkyl groups in **9**, **10**, and **12** to adopt the same bioactive conformation as the ethyl group in **2** or the propyl group in **3** with one branch of the chain. The energy penalties calculated in this way are 1.1, 1.9, and 3.1 kcal/mol for **9**, **10**, and **12**, respectively. If the relative affinities of these compounds are solely determined by the conformational energy penalties, these calculations predict that **9**, **10**, and **12** should have 6, 22, and 163 times lower affinities than their parent compounds **3**, **2**, and **3**, respectively. The experimental relative affinities are 11, 11, and 1444. Thus, the calculated conformational energy penalties for the assumed bioactive conformation of these compounds capture a major part of the observed relative affinities.

Properties of the Receptor Region in the Vicinity of the 6-Substituent (the "Interface" Region). According to the superimposition in Figure 2, the 6-position in the 4-quinolones corresponds to the 5′-position in the previously studied flavone series. Substitution in this position in the flavones by small substituents has, as mentioned above, been shown to result in a significant affinity increase.[11,12] As shown in Table 1, small alkyl substituents in the 6-position increase the affinity also in the 4-quinolone series. Ethyl (**2**), propyl (**17**), and isopropyl (**18**) substitution all increases the affinity by a factor 5 compared to that of the 6-unsubstituted compound **14**. In the flavone series, methyl substitution in the corresponding position increases the affinity by a factor of 6. The 6-bromo substituent in **16** increases the affinity by a factor of 5, which is a similar or slightly smaller substituent effect than is observed in the flavone series (a factor of 7−15).[12]

A significant difference between the substituent effect on the affinities in the flavone and the 4-quinolone series is observed for the 6-CF$_3$ substituent. In the previously studied flavone series[12] a CF$_3$ substituent in the 5′-position increases the affinity by a factor of 18, whereas there is essentially no effect on the affinity in the 4-quinolone series (**1** vs **14** in Table 1). This

Table 2. Affinity of Selected 4-Quinolones Tested on ^{3}H-Flumazenil Binding to $\alpha_1\beta_2\gamma_{2S}$ and $\alpha_3\beta_2\gamma_{2S}$ GABA$_A$ Receptor Subtypes

compound	R_1	R_2	R_3	X	$K_i\ \alpha_1$ (nM)[a]	$K_i\ \alpha_3$ (nM)[a]	K_i ratio: α_3/α_1
5	$CH_2CH_2CH(CH_3)_2$	H	CH_2CH_3	O	4.1 ± 2.6	89 ± 18	22
16	CH_2CH_3	H	Br	O	14 ± 7	26 ± 8	2
19	CH_2CH_3	H	$CH_2C_6H_5$	O	0.27 ± 0.06	7.2 ± 0.3	27
diazepam					12 ± 7	14 ± 10	1
zolpidem					53 ± 50	1850 ± 880	35

^{a} Each K_i value is the mean $\pm$ SD of three determinations. K_i for diazepam on α_1 is the mean $\pm$ SD of seven determinations.

indicates that the electronic properties of the aromatic ring induced by a polar substituent differ in the flavone and 4-quinoline systems and that the electronic properties of the aromatic ring to which the substituent is attached is of importance for the binding.

Albaugh et al. have shown that arylalkyl substituents such as a benzyl group could be introduced in a series of imidazopyridopyrimidinones resulting in compounds with high affinity for the benzodiazepine receptor.[19] According to pharmacophore modeling by Albaugh et al.[19] and the pharmacophore model in Figure 1b, the position of these substitutions in the imidazopyridopyrimidinones corresponds to the 6-position in the 4-quinolone moiety. This prompted us to synthesize and test the 6-benzyl compounds **19**, **20**, and **25**. Interestingly, the benzyl group in **19** increases the affinity by a factor of 56 compared to that of the 6-unsubstituted compound **14**. Replacing the ethyl ester group in **19** by a propyl ester giving **20** further increases the affinity by a factor of 8 leading to subnanomolar affinity ($K_i = 0.17$ nM). The replacement of the ethyl group in **3** by a benzyl group (**20**) increases the affinity by a factor of 10. Similarly, the replacement of the 6-ethyl group in **23** by a benzyl group giving **25** increases the affinity by a factor of 5, yielding the highest affinity compound in the present series of compounds ($K_i = 0.048$ nM).

Pyrazolopyrimidinones. The pyrazolopyrimidinones investigated in this study all display low affinities for the benzodiazepine site compared to those of the corresponding 4-quinolones. The low affinities are most probably due to larger desolvation energies for the pyrazolopyrimidones. The free energy of hydration for the pyrazolopyrimidone **27** was calculated to be -22 kcal/mol using AM1/SM2.[20] This should be compared to the calculated free energy of hydration for the 4-quinolone **14**, -17 kcal/mol. Thus, the desolvation energy of **28** is calculated to be 5 kcal/mol higher than that of **14**. The logP values for the two compounds as calculated by using the ClogP algorithm are -0.17 and 0.93 for **28** and **14**, respectively, indicating a significantly higher lipophilicity for **14** than for **28**.

Subtype Selectivity. A few compounds, **5**, **16**, and **19**, representing different types of substitution patterns were selected for testing on the GABA$_A$ receptor subtypes. The selection of **5** was based on the observation that the β-carboline BCCT which contains a *tert*-butyl ester group displays selectivity for $\alpha_1\beta_2\gamma_2$ over $\alpha_3\beta_2\gamma_2$ by a factor of 26, whereas the corresponding ethyl ester only displays low selectivity by a factor of 5.[9] According to pharmacophore modeling reported by He et al.,[9] the bulky *tert*-butyl group in BCCT interacts with the receptor in the L2 region. In terms of our pharmacophore model (Figure 1b), the bulky part of the 3-methylbutoxy group in **5** is proposed to interact with the receptor in the L2 region, making **5** an interesting candidate for a subtype selective compound.

As discussed above, compound **19** displays high affinity for the benzodiazepine receptor (Table 1). This in agreement with our expectations based on the effect observed by Albaugh et al. of benzyl substitution in imidazopyridopyrimidinones. In addition to their affinity increasing effect, some alkylaryl

substituents in the imidazopyridopyrimidinone series also displayed functional selectivity at receptor subtypes.[19] This made it of interest to test **19** on α_1 and α_3 containing receptors. Since compound **16** only has a small alkoxy substituent and a small substituent in the 6-position, it was selected as a reference compound.

The results given in Table 2 interestingly show that **5** as well as **19** display signicantly higher affinity for α_1 subunit-containing receptors compared to α_3 subunit-containing receptors. In contrast, the quinolone derivative **16** has essentially the same affinity for α_1- and α_3-containing receptors (Table 2). The ratio values ($K_i\ \alpha_3/K_i\ \alpha_1$) for **5** and **19** are in the same range as that of the well-known α_1 subunit selective compound zolpidem, but the affinities of **5** and **19** for $\alpha_1\beta_2\gamma_{2S}$ and $\alpha_3\beta_2\gamma_{2S}$ are significantly higher than those of zolpidem (Table 2). In terms of the pharmacophore model, these results indicate that selectivity for $\alpha_1\beta_2\gamma_{2S}$ over $\alpha_3\beta_2\gamma_{2S}$ may be achieved with appropriate substituents in the L2 region as well as in the receptor region in the vicinity of the 6-position in 4-quinolones (the "interface" region in Figure 1b).

Conclusions

The lead structure **1** has successfully been optimized with respect to affinity for the benzodiazepine receptor by using a pharmacophore-guided optimization approach. A number of high affinity compounds including compounds **20** and **23−25** displaying subnanomolar affinities have been obtained. These results validate the usefulness of the pharmacophore model. A few compounds were selected for testing on the $\alpha_1\beta_2\gamma_{2S}$ and $\alpha_3\beta_2\gamma_{2S}$ GABA$_A$ receptor subtypes. Two of the compounds (**5** and **19**) display selectivity for α_1- versus α_3-containing receptors by a factor of 22 and 27, respectively. These results demonstrate that selectivity for α_1- over α_3-containing receptors may be obtained via substituents interacting with the receptor in the L2 as well as in the "interface" region in terms of the pharmacophore model.

Experimental Section

Chemistry. ^{1}H and ^{13}C NMR were recorded at room temperature with a Bruker AR300 or a Bruker DR400 spectrometer. The spectra were recorded in CDCl$_3$, DMSO-d_6, and CD$_3$OD, and the solvent signals (7.27 and 77.0, 2.50 and 39.5, or 3.31 and 49.0 ppm, respectively) were used as reference. The raw data were transformed, and the spectra were evaluated with the standard Bruker UXNMR software (rev. 941001). Analytical thin-layer chromatography (TLC) was performed on Kiselgel 60 F$_{254}$ plates (Merck). Column chromatography was performed on SiO$_2$ (Matrex LC-gel: 60A, 35−70 MY, Grace). Melting points (uncorrected) were determined with a Reichert microscope. EI mass spectra were recorded at 70 eV with a JEOL S102 spectrometer, and ESI spectra were recorded with Micromass Q-TOF Micro. Compounds **1** and **25** were purchased from Maybridge.

Diethyl 4-Ethylanilinomethylenemalonate (2a). 4-Ethylaniline (0.145 g, 1.2 mmol) and diethyl ethoxymethylenemalonate (0.26 g, 1.2 mmol) were mixed and heated at 130 °C for 2 h. Low boiling components were evaporated at low pressure with a cold trap yielding **2a** (0.35 g, 1.2 mmol, quantitative yield), as a yellow oil.

3-Ethoxycarbonyl-6-ethyl-4-quinolone (2). 2a (0.756 g, 3.50 mmol) was added in portions to refluxing diphenyl ether (4 mL). The mixture was refluxed for 1 h and then allowed to cool to room temperature. Petroluem ether was added, and the resulting crystals were collected and washed with a large amount of petroleum ether. The crystals were purified by trituration with diethyl ether yielding **2** (0.320 g, 1.31 mmol, 37%), a white solid (mp: 271−273 °C). Anal. (C$_{14}$H$_{15}$NO$_3$) C, H, N.

6-Ethyl-3-propoxycarbonyl-4-quinolone (3). 2 (0.053 g, 0.22 mmol) and a catalytic amount of *p*-toluenesulfonic acid were dissolved in 25 mL of *n*-propanol. The mixture was refluxed overnight. A small amount of silica was added to the mixture followed by evaporation at reduced pressure. The crude product was purified by chromatography (CHCl$_3$:EtOH 9:1). The fractions containing the product (and the corresponding acid as a side product) were washed with sat. NaHCO$_3$(aq.) and dried with MgSO$_4$, yielding **3** (0.047 g, 0.18 mmol, 83%), a white solid (mp: 256−258 °C). Anal. (C$_{15}$H$_{17}$NO$_3$) C, H, N.

3-Butoxycarbonyl-6-ethyl-4-quinolone (4) was prepared and purified according to the procedure described for **3**, using *n*-butanol as solvent and reacting alcohol. The reaction yielded **4** (90%), a white solid (mp: 225−227 °C). Anal. (C$_{16}$H$_{19}$NO$_3$) C, H, N.

6-Ethyl-3-(3-methylbutoxycarbonyl)-4-quinolone (5) was prepared and purified according to the procedure described for **3**, using 3-methyl-1-butanol as solvent and reacting alcohol. The reaction yielded **5** (46%), a white solid (mp: 252−254 °C). Anal. (C$_{17}$H$_{21}$NO$_3$) C, H, N.

6-Ethyl-3-(2-methylbutoxycarbonyl)-4-quinolone (6) was prepared and purified according to the procedure described for **3**, using 2-methyl-1-butanol as solvent and reacting alcohol. The reaction yielded **6** (73%), a white solid (mp: 239−241 °C). Anal. (C$_{17}$H$_{21}$NO$_3$) C, H, N.

6-Ethyl-3-pentoxycarbonyl-4-quinolone (7). 2 (51 mg, 0.21 mmol) and a catalytic amount of Ti(O-*i*-Pr)$_4$ were dissolved in 10 mL of *n*-pentanol. The mixture was refluxed overnight. A small amount of silica was added to the mixture followed by evaporation at reduced pressure. The crude product was purified by chromatography (CHCl$_3$:EtOH 9:1) yielding **7** (49 mg, 0.172 mmol, 83%), a white solid (mp: 231−233 °C). Anal. (C$_{17}$H$_{21}$NO$_3$) C, H, N.

6-Ethyl-3-(2-ethylbutoxycarbonyl)-4-quinolone (8) was prepared and purified according to the procedure described for **3**, using 2-ethyl-1-butanol as solvent and reacting alcohol. The reaction yielded **8** (51%), a white solid (mp: 216−218 °C). Anal. (C$_{18}$H$_{23}$NO$_3$) C, H, N.

3-Cyclopentoxycarbonyl-6-ethyl-4-quinolone (9) was prepared and purified according to the procedure described for **7**, using cyclopentanol as solvent and reacting alcohol. The reaction yielded **9** (80%), a white solid (mp: 270−272 °C). Anal. (C$_{17}$H$_{19}$NO$_3$) C, H, N.

6-Ethyl-3-*i*-propoxycarbonyl-4-quinolone (10) was prepared and purified according to the procedure described for **7**, using *i*-propanol as solvent and reacting alcohol. The reaction yielded **10** (74%), a white solid (mp: 235−237 °C). Anal. (C$_{15}$H$_{17}$NO$_3$) C, H, N.

6-Ethyl-3-(4-methyl-2-pentoxycarbonyl)-4-quinolone (11) was prepared and purified according to the procedure described for **7**, using 4-methyl-2-butanol as solvent and reacting alcohol. The reaction yielded **11** (53%), a white solid (mp: 196−198 °C). Anal. (C$_{18}$H$_{23}$NO$_3$) C, H, N.

6-Ethyl-3-(3-pentoxycarbonyl)-4-quinolone (12) was prepared and purified according to the procedure described for **7**, using 3-pentanol as solvent and reacting alcohol. The reaction yielded **12** (43%), a white solid (mp: 231−232 °C). Anal. (C$_{17}$H$_{21}$NO$_3$) C, H, N.

3-Carboxy-6-ethyl-4-quinolone (13) was prepared and purified according to the procedure described for **3**, using the mixture *i*-propanol:H$_2$O (9:1) as solvent and water as the reacting species. The reaction yielded **13** (68%), a white solid (mp: 285−287 °C). Anal. (C$_{12}$H$_{11}$NO$_3$) C, H, N.

Diethyl anilinomethylenemalonate (14a) was prepared according to the procedure described for **2a**, using aniline as reacting amine. The crude product was purified by recrystallization from diethyl ether yielding **14a** (82%), a white solid (mp: 49−51 °C).

3-Ethoxycarbonyl-4-quinolone (14) was prepared and purified according to the procedure described for **2**, starting from **14a**. The reaction yielded **14** (43%), a white solid (mp: 270−272 °C). Anal. (C$_{12}$H$_{11}$NO$_3$) C, H, N.

3-Butoxycarbonyl-4-quinolone (15) was prepared and purified according to the procedure described for **3**, starting from **14** and using *n*-butanol as solvent and reacting alcohol. The reaction yielded **15** (89%), a white solid (mp: 252−254 °C). Anal. (C$_{14}$H$_{15}$NO$_3$) C, H, N.

Diethyl 4-bromoanilinomethylenemalonate (16a) was prepared according to the procedure described for **2a**, using 4-bromoaniline as reacting amine. The crude product was purified by recrystallization from diethyl ether yielding **16a** (73%), a white solid (mp: 93−95 °C).

6-Bromo-3-ethoxycarbonyl-4-quinolone (16) was prepared and purified according to the procedure described for **2**, starting from **16a**. The reaction yielded **16** (57%), a white solid (mp: 320−322 °C). Anal. (C$_{12}$H$_{10}$NO$_3$Br) C, H, N.

Diethyl 4-propylanilinomethylenemalonate (17a) was prepared according to the procedure described for **2a**, using 4-*n*-propylaniline as reacting amine. Low boiling components were evaporated yielding **17a** (quantitative), a white solid (mp: 43−45 °C).

3-Ethoxycarbonyl-6-propyl-4-quinolone (17) was prepared and purified according to the procedure described for **2**, starting from **17a**. The reaction yielded **17** (74%), a white solid (mp: 268−270 °C). Anal. (C$_{15}$H$_{17}$NO$_3$) C, H, N.

Diethyl 4-*i*-propylanilinomethylenemalonate (18a) was prepared according to the procedure described for **2a**, using 4-isopropylaniline as reacting amine. Low boiling components were evaporated yielding **18a** (quantitative), a brown oil.

3-Ethoxycarbonyl-6-*i*-propyl-4-quinolone (18) was prepared and purified according to the procedure described for **2**, starting from **18a**. The reaction yielded **18** (43%), a white solid (mp: 271−273 °C). Anal. (C$_{15}$H$_{17}$NO$_3$) C, H, N.

Diethyl 4-benzylanilinomethylenemalonate (19a) was prepared according to the procedure described for **2a**, using 4-benzylaniline as reacting amine. Low boiling components were evaporated yielding **19a** (quantitative) as a brown oil.

6-Benzyl-3-ethoxycarbonyl-4-quinolone (19) was prepared and purified according to the procedure described for **2**, starting from **19a**. The reaction yielded **19** (87%), a white solid (mp: 278−280 °C). Anal. (C$_{19}$H$_{17}$NO$_3$) C, H, N.

6-Benzyl-3-propoxycarbonyl-4-quinolone (20) was prepared and purified according to the procedure described for **7**, starting from **19** and using *n*-propanol as solvent and reacting alcohol. The reaction yielded **20** (66%), a white solid (mp: 273−275 °C). Anal. (C$_{20}$H$_{19}$NO$_3$) C, H, N.

Diethyl 4-ethylanilinoethylidenemalonate (21a). 4-Ethylaniline (80.4 mg, 0.663 mmol), diethyl acetylmalonate (0.134 g, 0.334 mmol), and a catalytic amount of *p*-toluenesulfonic acid were refluxed in 10 mL of pentane. Water produced during the reaction was removed using a Dean−Stark trap filled with 4 Å molecular sieves. After 24 h, 5 mL of sat. NaHCO$_3$(aq) was added and the mixture was extracted with diethyl ether (210 mL). The combined organic extract was dried with MgSO$_4$. The crude product was purified by chromatography (SiO$_2$, petroleum ether:ethyl acetate 6:1−1:1) yielding **21a** (102 mg, 0.334 mmol, 50%), a yellow solid (mp: 54−56 °C).

3-Ethoxycarbonyl-6-ethyl-2-methyl-4-quinolone (21) was prepared and purified according to the procedure described for **2**, starting from **21a**. The reaction yielded **21** (27%), a white solid (mp: 248−250 °C). Anal. (C$_{15}$H$_{17}$NO$_3$) C, H, N.

Diethyl 4-bromoanilinoethylidenemalonate (22a) was prepared and purified according to the same procedure described for **21a**, using 4-bromoaniline as reacting amine. The reaction yielded **22a** (35%), a white solid (mp: 61−63 °C).

6-Bromo-3-ethoxycarbonyl-2-methyl-4-quinolone (22) was prepared and purified according to the procedure described for **2**,

starting from **22a**. The reaction yielded **22** (45%), a white solid (mp: 271−273 °C). Anal. ($C_{13}H_{12}NO_3Br$) C, H, N.

6-Ethyl-3-propylaminocarbonyl-4-quinolone (23) was prepared and purified according to the procedure described for **7**, using *n*-propylamine as solvent and reacting amine. The reaction yielded **23** (64%), a white solid (mp: 205−207 °C). Anal. ($C_{15}H_{18}N_2O_2$) C, H, N.

3-Butylaminocarbonyl-6-ethyl-4-quinolone (24) was prepared and purified according to the procedure described for **7**, using *n*-butylamine as solvent and reacting amine. The reaction yielded **24** (92%), a white solid (mp: 180−182 °C). Anal. ($C_{16}H_{20}N_2O_2$) C, H, N.

6-Benzyl-3-propylaminocarbonyl-4-quinolone (25) was prepared and purified according to the procedure described for **7**, using *n*-propylamine as solvent and reacting amine. The reaction yielded **25** (76%), a white solid (mp: 209−211 °C). Anal. ($C_{20}H_{20}N_2O_2$) C, H, N.

Propyl 2-methyl-7-oxo-4,7-dihydropyrazolo[1,5-*a*]pyrimidine-6-carboxylate (27) was prepared according to the procedure described for **7**, starting from **26** and using *n*-propanol as solvent and reacting alcohol. The crude product was purified by chromatography (CH_2Cl_2:MeOH 8:1) yielding **27** (quantitative yield), a white solid (mp: 267−269 °C). Anal. ($C_{11}H_{13}N_3O_3$) C, H, N.

Ethyl 7-Oxo-4,7-dihydropyrazolo[1,5-*a*]pyrimidine-6-carboxylate (28). 3-Aminopyrazole (432 mg, 5.2 mmol) was dissolved in diethyl ethoxymethylenemalonate (1.12 g, 5.2 mmol) and heated at 200 °C for 10 min. The crude product was purified by recrystallization from DMF and filteration on silica (CH_2Cl_2:EtOH 10:1), yielding **28** (630 mg, 3.04 mmol, 58.5%), a white solid (mp: 295−296 °C). Anal. ($C_9H_9N_3O_3$) C, H, N.

Propyl 7-oxo-4,7-dihydropyrazolo[1,5-*a*]pyrimidine-6-carboxylate (29) was prepared according to the procedure described for **7**, starting from **28** and using *n*-propanol as solvent and reacting alcohol. The crude product was purified by chromatography (CH_2Cl_2:EtOH 10:1) yielding **29** (89%), a white solid (dec: 300 °C). Anal. ($C_{10}H_{11}N_3O_3$) C, H, N.

Benzodiazepine Receptor Binding in Vitro. Binding of ³H-flumazenil (87 Ci/mmol) to rat cortical membranes and to a membrane suspension of HEK 293 cells expressing human $\alpha_1\beta_2\gamma_{2S}$ or $\alpha_3\beta_2\gamma_{2S}$ $GABA_A$ receptors was done following methods previously described by Kahnberg et al.[12] In brief, tissue is homogenized in 20 mL of Tris, HCl (30 mM, pH 7.4) using an Ultra-Turrax homogenizer. The suspensions are centrifuged at 27000*g* for 15 min followed by three centrifugation resuspension cycles. The washed pellet is resuspended in 20 mL of buffer, incubated at 37 °C for 30 min, and then centrifuged for 10 min (27000*g*). The pellet is washed once, and the final pellet is resuspended in 30 mL of Tris-HCl buffer (50 mM, pH 7.4) and stored at −20 °C until use. For binding studies frozen membrane suspensions were thawed and centrifuged (27000*g*, 10 min). The pellet was resuspended into Tris-citrate buffer (50 mM, pH 7.1) at a tissue concentration: cortex preparation ca. 50 μg protein/0.55 mL assay (1 mg original tissue/ 0.55 mL assay) and HEK cells ca. 25 μg protein per 0.55 mL assay. Aliquots of 0.5 mL of membrane preparation are added to 25 μL of ³H-flumazenil solution (1 nM final concentration) and 25 μL containing test substance and incubated at an ice-bath (0−4 °C) for 40 min. The incubated samples were added to 5 mL of ice-cold buffer (Tris-citrate, 50 mM, pH 7.1), poured directly onto Whatman GF/C glass fiber filters under suction, and immediately washed with 5 mL of ice-cold buffer. Nonspecific binding was determined by adding clonazepam (1 μM final concentration) to separate samples. Protein was estimated by conventional protein assay method using bovine serum albumin as standard.

IC$_{50}$ values were determined using four to six different concentrations of test substance. K_i values were calculated according to $K_i = IC_{50}/(1 + [L]/K_D)$, ([L] is the concentration of ³H-flumazenil; K_D is binding affinity constant of ³H-flumazenil (1.6 nM). All assays were done in triplicate (cortical assays) or duplicate (HEK cells).

Computational Methods. Conformational analyses were performed by using the Monte Carlo Multiple Minimum (MCMM) method[21] with the default setting as implemented in MacroModel 7.0.[22] Force field calculations were carried out using the MMFF94s force field[23] with solvation effects calculated by the GB/SA hydration model.[24] The energy minimizations were carried out using the Polak−Ribiere conjugate gradient algorithm (PRCG) as implemented in MacroModel 7.0. LogP calculations were performed by using the ClogP algorithm as implemented in ChemDrawUltra version 8.0.3 (CambridgeSoft). The free energies of hydration for compounds **14** and **27** were calculated by using AM1/SM2[20] as implemented in Spartan 02 for Macintosh (Wavefunction, Inc.)

Supporting Information Available: Spectral data (¹H NMR, ¹³C NMR and HRMS) of all synthesized compounds and elemental analysis for all new target compounds. This material is available free of charge via the Internet at http://pubs.acs.org.

References

(1) Sieghart, W. Structure and pharmacology of gamma-aminobutyric acid A receptor subtypes. *Pharmacol. Rev.* **1995**, *47* (2), 181−234.

(2) Kaupmann, K.; Huggel, K.; Heid, J.; Flor, P. J.; Bishoff, S.; Mickel, S. J.; McMaster, G.; Angst, C.; Bittiger, H.; Froestl, W.; Bettler, B., Expression cloning of GABA$_B$ receptors uncovers similarity to metabotropic glutamate receptors. *Nature* **1997**, *386*, 239−246.

(3) Rabow, L. E.; Russek, S. H.; Farb, D. H. From ion currents to genomic analysis: Recent advances in GABA$_A$ receptor research. *Synapse* **1995**, *21*, 189−274.

(4) Johnston, G. A. R. GABA$_C$ receptors: relatively simple transmitter-gated ion channels. *Trends Pharmacol. Sci.* **1996**, *17*, 319−323.

(5) Barnard, E.; Skolnick, P.; Olsen, R.; Mohler, H.; Sieghart, W.; Biggio, G.; Braestrup, C.; Bateson, A.; Langer, S., International union of pharmacology. XV. Subtypes of γ-aminobutyric acid$_A$ receptors: Classification of the basis of subunit structure and receptor function. *Pharmacol. Rev.* **1998**, *50*, 291−313.

(6) Rudolph, U.; Crestani, F.; Benke, D.; Brunig, I.; Benson, J. A.; Fritschy, J. M.; Martin, J. R.; Bluethmann, H.; Mohler, H. Benzodiazepine actions mediated by specific gamma-aminobutyric acid-(A) receptor subtypes. *Nature* **1999**, *401* (6755), 796−800.

(7) Rudolph, U.; Crestani, F.; Mohler, H. GABA$_A$ receptor subtypes: dissecting their pharmacological functions. *Trends Pharmacol. Sci.* **2001**, *22*, 188−194.

(8) Doble, A.; Martin, I. L. *The GABA$_A$/Benzodiazepine receptor as Target for Psychoactive Drugs*; Springer-Verlag: Heidelberg, Germany, 1996.

(9) He, X.; Huang, Q.; Ma, C.; Yu, S.; McKernan, R.; Cook, J. M. Pharmacophore/receptor models for GABA$_A$/BzR $\alpha2\beta3\gamma2$, $\alpha3\beta3\gamma2$ and $\alpha4\beta3\gamma2$ recombinant subtypes. Included volume analysis and comparison to $\alpha1\beta3\gamma2$, $\alpha5\beta3\gamma2$ and $\alpha6\beta3\gamma2$ subtypes. *Drug Des. Discovery* **2000**, *17* (2), 131−171.

(10) Gardner, C. R.; Tully, W. R.; Hedgecock, J. R. The rapidly expanding range of neuronal benzodiazepine ligands. *Prog. Neurobiol.* **1993**, *40*, 1−61.

(11) Dekermendijan, K.; Kahnberg, P.; Witt, M.; Sterner, O.; Nielsen, M.; Liljefors, T. Structure−activity relationship and molecular modeling analysis of flavonoids binding to the benzodiazepine site of the rat brain GABA$_A$ receptor complex. *J. Med. Chem.* **1999**, *42*, 4343−4350.

(12) Kahnberg, P.; Lager, E.; Rosenberg, C.; Schougaard, J.; Camet, L.; Sterner, O.; Østergaard Nielsen, E.; Nielsen, M.; Liljefors, T. Refinement and evaluation of a pharmacophore model for flavone derivatives binding to the benzodiazepine site of the GABA$_A$ receptor. *J. Med. Chem.* **2002**, *45*, 4188−4201.

(13) Zhang, W.; Koehler, K. F.; Zhang, P.; Cook, J. M., Development of a comprehensive pharmacophore model for the benzodiazepine receptor. *Drug Des. Discovery* **1995**, *12*, 193−248.

(14) Kahnberg, P.; Howard, M.; Liljefors, T.; Nielsen, M.; Østergaard Nielsen, E.; Sterner, O.; Pettersson, I. The use of a pharmacophore model for identification of novel ligands for the benzodiazepine binding site of the GABA$_A$ receptor. *J. Mol. Graphics Modelling* **2004**, *23*, 253−261.

(15) Gould, G.; Jacobs, W. The synthesis of certain substituted quinolines and 5,6-benzoquinolines. *J. Am. Chem. Soc.* **1939**, *61*, 2890−2895.

(16) Seebach, D.; Hungerbühler, E.; Naef, R.; Schnurrenberger, P.; Weidmann, B.; Züger, M. Titanate-mediated trans-esterifications with functionalized substrates. *Synthesis* **1982**, *13*, 138−141.

(17) Nagahara, K.; Kawano, H.*;* Sasaoka, S.; Ukawa, C.; Hirama, T.; Takada, A.; Cottam, H. B.; Robins, R. K. Reaction of 5-aminopyrazole derivatives with ethoxymethylenemalononitrile and its analogues. *J. Heterocycl. Chem.* **1994**, *31*, 239−243.

(18) Albaugh, P. A.; Currie, K. S.; Rosewater, D.; Cai, G. Substituted 4-oxo-Quinoline-3-carboxamides: GABA Brain Receptor Ligands. Patent Application WO 2000/68202.

(19) Albaugh, P. A.; Marshall, L.; Gregory, J.; White, G.; Hutchison, A.; Ross, P. C.; Gallagher, D. W.; Tallman, J. F.; Crago, M.; Casella, J. V. Synthesis and biological evaluation of 7,8,9,10-tetrahydroimidazo-[1,2-*c*]pyrido[3,4-*e*]pyrimidin-5(6*H*)-ones as functionally selective ligands of the benzodiazepine receptor site on the GABA_A receptor. *J. Med. Chem.* **2002**, *45*, 5043−5051.

(20) Cramer, C. J.; Truhlar, D. G. AM1-SM2 and PM3-SM3 parametrized SCF solvation models for free energies in aqueous solution. *J. Comput.-Aided Mol. Des.* **1992**, *6*, 629−666.

(21) Chang, G.; Guida, W. C.; Still, W. C. An Internal Coordinate Monte Carlo Method for Searching Conformational Space. *J. Am. Chem. Soc.* **1989**, *111*, 4379−4386.

(22) Mohamadi, F.; Richards, N. G. J.; Guida, W. C.; Liskamp, R.; Lipton, M.; Caulfield, C.; Chang, G.; Hendrickson, T.; Still, W. C. Macro-Model − An Integrated Software System for Modeling Organic and Bioorganic Molecules Using Molecular Mechanics. *J. Comput. Chem.* **1990**, *11*, 440−467.

(23) Halgren, T. A. MMFF94s option for energy minimization studies. *J. Comput. Chem.* **1999**, *29*, 720−729.

(24) Still, W. C.; Tempczyk, A.; Hawley, R. C.; Hendrickson, T. Semianalytical Treatment of Solvation for Molecular Mechanics and Dynamics. *J. Am. Chem. Soc.* **1990**, *112*, 6127−6129.